Article

The Dinuclear Zn(II) Complex Catalyzed Cyclization of a Series of 2-Hydroxypropyl Aryl Phosphate RNA Models: Progressive Change in Mechanism from Rate-Limiting P–O Bond Cleavage to Substrate Binding

Shannon E. Bunn, C. Tony Liu, Zhong-Lin Lu, Alexei A. Neverov, and R. Stan Brown

J. Am. Chem. Soc., **2007**, 129 (51), 16238-16248 • DOI: 10.1021/ja076847d

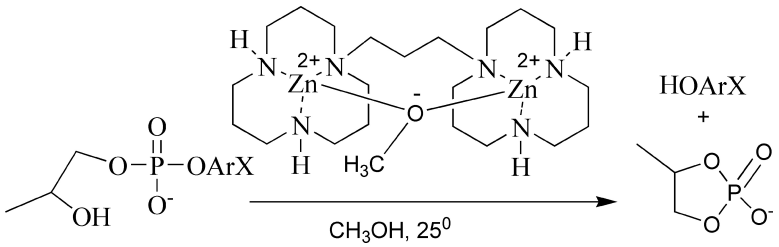

More About This Article

Additional resources and features associated with this article are available within the HTML version:

- Supporting Information
- Links to the 9 articles that cite this article, as of the time of this article download
- Access to high resolution figures
- Links to articles and content related to this article
- Copyright permission to reproduce figures and/or text from this article

View the Full Text HTML

J|A|C|S
ARTICLES
Published on Web 11/30/2007

The Dinuclear Zn(II) Complex Catalyzed Cyclization of a Series of 2-Hydroxypropyl Aryl Phosphate RNA Models: Progressive Change in Mechanism from Rate-Limiting P−O Bond Cleavage to Substrate Binding

Shannon E. Bunn, C. Tony Liu, Zhong-Lin Lu,† Alexei A. Neverov, and R. Stan Brown*

Contribution from the Department of Chemistry, Queen's University, Kingston, Ontario, Canada K7L 3N6

Received September 10, 2007; E-mail: rsbrown@chem.queensu.ca

Abstract: A methoxide-bridged dinuclear Zn(II) complex of 1,3-[*N,N′-bis*(1,5,9-triazacyclododecane)]propane (**1**-Zn(II)$_2$:($^-$OCH$_3$)) was prepared, and its catalysis of the cyclization of a series of 2-hydroxypropyl aryl phosphates (**4**a−g) was investigated in methanol at ^s_spH 9.8, $T = 25$ °C by stopped-flow spectrophotometry. An X-ray diffraction structure of the hydroxide analogue of **1**-Zn(II)$_2$:($^-$OCH$_3$), namely **1**-Zn(II)$_2$:($^-$OH), reveals that each of the Zn(II) ions is coordinated by the three N's of the triazacyclododecane units and a bridging hydroxide. The cyclizations of substrates **4**a−g reveal a progressive change in the observed kinetics from Michaelis−Menten saturation kinetics for the poorer substrates (4-OCH$_3$ (**4**g); 4-H (**4**f); 3-OCH$_3$ (**4**e); 4-Cl (**4**d); 3-NO$_2$, (**4**c)) to second-order kinetics (linear in **1**-Zn(II)$_2$:($^-$OCH$_3$)) for the better substrates (4-NO$_2$,3-CH$_3$ (**4**b); 4-NO$_2$, (**4**a)). The data are analyzed in terms of a multistep process whereby a first formed complex rearranges to a reactive complex with a doubly activated phosphate coordinated to both metal ions. The kinetic behavior of the series is analyzed in terms of change in rate-limiting step for the catalyzed reaction whereby the rate-limiting step for the poorer substrates (**4**g−c) is the chemical step of cyclization of the substrate, while for the better substrates (**4**b,a) the rate-limiting step is binding. The catalysis of the cyclization of these substrates is extremely efficient. The k_{cat}/K_M values for the catalyzed reactions range from 2.75×10^5 to 2.3×10^4 M^{-1} s^{-1}, providing an acceleration of 1×10^8 to 4×10^9 relative to the methoxide reaction (k_2^{OCH3}, which ranges from 2.6×10^{-3} to 5.9×10^{-6} M^{-1} s^{-1} for **4**a−g). At a ^s_spH of 9.8 where the catalyst is maximally active, the acceleration for the substrates ranges from $(1 - 4) \times 10^{12}$ relative to the background reaction at the same ^s_spH. Detailed energetics calculations show that the transition state for the catalyzed reaction comprising **1**-Zn(II)$_2$, methoxide, and **4** is stabilized by about −21 to −23 kcal/mol relative to the transition state for the methoxide reaction. The pronounced catalytic activity is attributed to a synergism between a positively charged catalyst that has high affinity for the substrate and for the transition state for cyclization, and a medium effect involving a reduced polarity/dielectric constant that complements a reaction where an oppositely charged reactant and catalyst experience charge dispersal in the transition state.

1. Introduction

Intense effort has been devoted to the study of model systems for the cleavage of phosphodiesters mediated by simple mono- and dinuclear metal ion complexes.[1] Much of this work has been driven by the fact that phosphodiesters are extremely stable entities well suited for the storage of genetic information in RNA and DNA, and yet Nature has provided Zn^{2+}-containing enzymes that accelerate their cleavage by impressive factors of up to 10^{16}-fold.[2] Our own work involved investigation of systems comprising mono- and dinuclear Zn(II)- and Cu(II)-containing complexes of 1,5,9-triazacyclododecane and 1,3-bis-N_1-(1,5,9-triazacyclododecyl)propane (**1**) in methanol[3] and Zn(II) in ethanol[4] where the reduced polarity media help to promote the cleavage of a well-studied RNA model, namely 2-hydroxypropyl *p*-nitrophenyl phosphate (**2**). The most notable aspect of this work relates to the very effective catalysis achieved for the cleavage of **2** promoted by **1**-Zn(II)$_2$ in the presence of one equivalent of methoxide in methanol (which produces the

† Present address: Beijing Normal University, College of Chemistry, Beijing, China 100875. E-mail: luzl@bnu.edu.cn.

(1) (a) Mancin, F.; Tecillia, P. *New J. Chem.*, **2007**, *31*, 800. (b) Weston, J. *Chem. Rev.* **2005**, *105*, 2151. (c) Molenveld, P.; Engbertsen, J. F. J.; Reinhoudt, D. N. *Chem. Soc. Rev.* **2000**, *29*, 75. (d) Williams, N. H.; Takasaki, B.; Wall, M.; Chin, J. *Acc. Chem. Res.* **1999**, *32*, 485. (e) Mancin, F.; Scrimin, P.; Tecilla, P.; Tonellato, U. *Chem. Commun.* **2005**, 2540. (f) Morrow, J. R.; Iranzo, O. *Curr. Opin. Chem. Biol.* **2004**, *8*, 192.

(2) (a) Cowan, J. A. *Chem. Rev.* **1998**, *98*, 1067. (b) Wilcox D. E. *Chem. Rev.* **1996**, *96*, 2435. (c) Sträter, N.; Lipscomb, W. N.; Klabunde, T.; Krebs, B. *Angew. Chem., Int. Ed. Engl.* **1996**, *35*, 2024.

(3) (a) Neverov, A. A.; Lu, Z.-L.; Maxwell, C. I.; Mohamed, M. F.; White, C. J.; Tsang. J. S. W.; Brown, R. S. *J. Am. Chem. Soc.* **2006**, *128*, 16398. (b) Lu, Z.-L.; Liu, C. T.; Neverov, A. A.; Brown, R. S. *J. Am. Chem. Soc.* **2007**, *129*, 11642.

(4) Liu, C. T.; Neverov, A. A.; Brown, R. S. *Inorg. Chem.* **2007**, *46*, 1778.

10.1021/ja076847d CCC: $37.00

Scheme 1 [a]

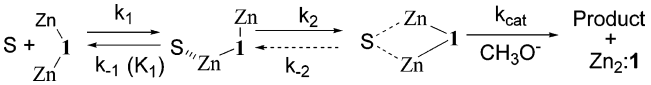

[a] S = phosphodiester substrate, charges omitted for simplicity.

complex **1**-Zn(II)$_2$:($^-$OCH$_3$) and sets the ^s_spH[5] of the medium at 9.4−9.8) where the second-order rate constant (k_2^{obs}) of 275,000 M^{-1} s^{-1} is several orders of magnitude larger than anything reported to date for related catalysts in water.[3a,6−8] This result demands further investigation when viewed in the light of the **1**-Zn(II)$_2$:($^-$OCH$_3$)-promoted catalysis of cleavage of a DNA model, methyl *p*-nitrophenyl phosphate (**3**), where the plot of

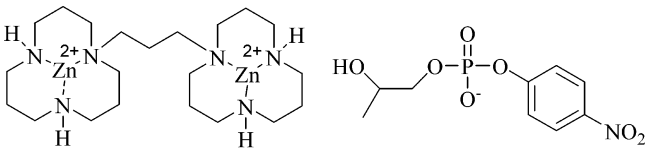

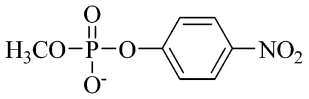

3

k_{obs} vs [**1**-Zn(II)$_2$:($^-$OCH$_3$)]$_{free}$ exhibited Michaelis−Menten behavior with K_M and k_{max} values of 0.37 ± 0.07 mM and (4.1 ± 0.3) × 10^{-2} s^{-1}, respectively.[3a] That two closely related substrates exhibited such different kinetic behavior led us to propose the mechanism given in Scheme 1 where the rate-limiting step with **2** was its binding (k_1 or k_2), whereas in the case of the slower-reacting **3** it was the chemical step of cleavage of the bound substrate (k_{cat}) to release *p*-nitrophenol.

We recently reported that the cleavages of **2** and **3** promoted by the corresponding Cu(II)$_2$ complex, **1**-Cu(II)$_2$:($^-$OCH$_3$),[3b] follow a pathway similar to the mechanism given in Scheme 1. However, there are sufficient differences in the chemical, physical, and coordination properties of the two metal ions that one might wonder about the general similarity of their catalytic processes. A better test for the proposed scheme requires study of the **1**-Zn(II)$_2$:($^-$OCH$_3$)-catalyzed cleavage of a series of hydroxypropyl aryl phosphates where the rate of the chemical cleavage step (k_{cat}) can be altered by changing the nature of the departing aryloxy group. In the following we report a kinetic study of the cleavage of such a series of substrates (**4**a−g) promoted by **1**-Zn(II)$_2$:($^-$OCH$_3$) where there is a gradual change from Michaelis−Menten kinetics to second-order kinetics as the ^s_spK_a of the leaving phenol group is decreased. In addition, we report a detailed analysis that shows the energies associated with the various steps of methoxide binding to the catalyst, subsequent substrate binding, and activation energies for the catalytic steps with substrates **4**a−g which are compared with the methoxide promoted reactions.

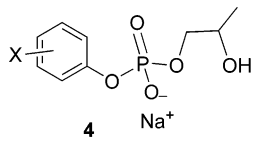

4

4a (**2**). X = 4-NO$_2$
b. X = 4-NO$_2$, 3-CH$_3$
c. X = 3-NO$_2$
d. X = 4-Cl
e. X = 3-OCH$_3$
f. X = H,
g. X = 4-OCH$_3$

2. Experimental

2.1. Materials. Methanol (99.8% anhydrous), sodium methoxide (0.50 M solution in methanol, titrated against N/50 certified standard aqueous HCl solution and found to be 0.49 M), tetrabutylammonium hydroxide in methanol (1 M, titrated against N/50 certified standard aqueous HCl solution and found to be 1.087 M), Zn(CF$_3$SO$_3$)$_2$, *p*-nitrophenol (98%), 4-chlorophenol (99+%), 3-nitrophenol (99%), 3-methyl-4-nitrophenol (98%), phenol (99%), 4-methoxyphenol (99%), 3-methoxyphenol (96%), triethylamine (≥99.5%), propylene oxide (ReagentPlus, 99%), phosphorus oxychloride (99%), and Ba(OH)$_2$ were purchased from Aldrich and used without further purification. HClO$_4$ (70% aqueous solution, titrated to be 11.40 M) was purchased from Acros Organics and used as supplied. The sodium salts of all the 2-hydroxylpropyl aryl phosphates were prepared by a modification[9] of a prior procedure.[10] The corresponding disodium salts of the aryl monophosphates required for the preparation of **4**a−g were synthesized according to a literature procedure.[11] Each of **4**a−g had ^{1}H NMR, ^{31}P NMR, and exact MS spectra consistent with those of the structure (see the Supporting Information). 1,3-Bis-*N*$_1$-(1,5,9-triazacyclododecyl)-propane (**1**) was prepared as described.[12] The dinuclear **1**-Zn(II)$_2$:($^-$OCH$_3$) complex was prepared as a 2.5 mM stock solution in anhydrous methanol at 25 °C by sequential addition of aliquots of stock solutions of sodium methoxide, 1,3-bis-*N*$_1$-(1,5,9-triazacyclododecyl)propane, and Zn(CF$_3$SO$_3$)$_2$ such that the relative ratios were 1:1:2. This order of addition is essential for the formation of the catalyst complex which takes ~40 min in methanol (as monitored by the change in catalytic activity over time).

2.2. Methods. ^{1}H NMR and ^{31}P NMR spectra were determined at 400 and 162.04 MHz. The CH$_3$OH$_2^+$ concentrations were determined potentiometrically using a combination glass electrode (Radiometer model no. XC100-111-120-161) calibrated with certified standard aqueous buffers (pH = 4.00 and 10.00) as described in previous papers.[13] The ^s_spH values in methanol were determined by subtracting the correction constant of −2.24[13a] from the readings obtained from the electrode, and the autoprotolysis constant for methanol was taken to be 10$^{-16.77}$ M^2. The ^s_spH values for the kinetic experiments were simply measured from solutions containing the complex and generally found to be in the range of 9.8 ± 0.2 at the concentrations of catalyst employed. We have found that the addition of buffers to control the ^s_spH inhibits the catalytic reaction, probably due to the associated counterions that bind to the catalyst, and thus, all the kinetic studies were done under buffer-free conditions. The first and second macroscopic ^s_spK_a values for **1**:Zn$_2$:(HOCH$_3$) and **1**:Zn$_2$:(HOCH$_3$)($^-$OCH$_3$) (0.4 mM) were determined to be 9.41 ± 0.01[3b] and 10.11 ± 0.01 from duplicate measurements of the ^s_spH at half neutralization, whereby the [**1**-Zn(II)$_2$:($^-$OCH$_3$)]/[**1**-Zn(II)$_2$:(HOCH$_3$)] or [**1**-Zn(II)$_2$:($^-$OCH$_3$)$_2$]/

(5) For the designation of pH in nonaqueous solvents we use the forms recommended by the IUPAC, *Compendium of Analytical Nomenclature: Definitive Rules 1997*, 3rd ed.; Blackwell: Oxford, U.K. 1998. If one calibrates the measuring electrode with aqueous buffers and then measures the pH of an aqueous buffer solution, the term ^w_wpH is used; if the electrode is calibrated in water and the pH of the neat buffered methanol solution is then measured, the term ^s_wpH is used; and if the electrode is calibrated in the same solvent and the pH reading is made, then the term ^s_spH is used. Since the autoprotolysis constant of methanol is 10$^{-16.77}$, neutral ^s_spH is 8.4.

(6) Feng, G.; Mareque-Rivas, J. C.; Williams, N. H. *Chem. Commun.* **2006**, 1845.
(7) Feng, G.; Natale, D.; Prabaharan, R.; Mareque-Rivas, J. C.; Williams, N. H. *Angew. Chem., Int. Ed.* **2006**, *45*, 7056.
(8) Iranzo, O.; Kovalevsky, A. Y.; Morrow, J. R.; Richard, J. P. *J. Am. Chem. Soc.* **2003**, *125*, 1988.
(9) Tsang, J. S.; Neverov, A. A.; Brown, R. S. *J. Am. Chem. Soc.* **2003**, *125*, 1559.
(10) Brown, D. M.; Usher, D. A. *J. Chem. Soc.* **1965**, 6558.
(11) Williams, A.; Naylor, R. A. *J. Chem. Soc. (B)* **1971**, *10*, 1973.
(12) Kim, J.; Lim, H. *Bull. Korean Chem. Soc.* **1999**, *20*, 491.
(13) (a) Gibson, G.; Neverov, A. A.; Brown, R. S. *Can. J. Chem.* **2003**, *81*, 495. (b) Gibson, G. T. T.; Mohamed, M. F.; Neverov, A. A.; Brown, R. S. *Inorg. Chem.* **2006**, *45*, 7891.

[**1**-Zn(II)$_2$:($^-$OCH$_3$)] ratios were 1.0. The half neutralization involved treating a 0.4 mM methanol solution of **1**-Zn(II)$_2$:($^-$OCH$_3$), prepared as described in the Materials section above, with 0.5 equiv of $HClO_4$ or $NaOCH_3$ (diluted to a 0.05 M stock solution in anhydrous methanol) and measuring the ^s_spH.

2.3. Stopped-Flow Kinetics in Methanol. A 2.5 mM stock solution of **1**-Zn(II)$_2$:($^-$OCH$_3$) in methanol was prepared in an oven-dried vial, stoppered with a needle-permitting lid, and then sealed with Parafilm under nitrogen gas. This solution was used to prepare stock catalyst solutions of concentrations ranging from 0.4 mM < [**1**-Zn(II)$_2$:($^-$OCH$_3$)] < 2.5 mM, which were loaded into one syringe of the stopped-flow reaction analyzer. Substrate stock solutions at concentrations of 8×10^{-5} M (for **4**b−e) and 1.6×10^{-4} M (for **4**f,g) were prepared and loaded into the second syringe. The final respective substrate concentrations were 4×10^{-5} M (**4**b−e) and 8×10^{-5} M (**4**f,g). At each concentration five kinetic runs were recorded, and the average values were used for the k_{obs} for appearance of phenol product vs [catalyst] plots. The production of the phenol was monitored at the following wavelengths: **4**b, 323 nm; **4**c, 340 nm; **4**d, 284 nm; **4**e, 282 nm; **4**f, 280 nm; **4**g, 292 nm.

The $^s_s pK_a$ values in methanol of the corresponding phenol leaving group for **4**a, **4**c, **4**d, **4**f, and **4**g were obtained from previous work[14] and were plotted against the known $^s_s pK_a$ values in water and fit by linear regression to the relationship, $^s_s pK_a^{MeOH} = (1.09 \pm 0.06)\ pK_a^{HOH} + (3.40 \pm 0.50)$. This relationship was used to interpolate the $^s_s pK_a$ values in methanol for the **4**b and **4**e phenols.

The base-dependence of the **1**:Zn(II)$_2$-catalyzed cyclization of **4**f was studied through "pH jump" experiments. The concentration of the initially prepared catalyst (**1**-Zn(II)$_2$:($^-$OCH$_3$)) was held constant at 0.8 mM, and the initial concentration of **4**f was 8×10^{-5} M. To the solution containing **4**f, a required amount of perchloric acid or sodium methoxide was added such that when mixed in the stopped-flow reaction analyzer for rapid monitoring of the change in absorbance at 280 nm, the [CH_3O^-]/[**1**:Zn$_2$] ratio was varied from 0 through 2.

Base-catalyzed reactions were also conducted for each of **4**b−g. Tetrabutylammonium hydroxide (1.087 M in methanol) was used as the base, and it was assumed to be completely converted to tetrabutylammonium methoxide in methanol. For each substrate, the reaction media were prepared in duplicate with at least three concentrations in the range of 0.02−0.3 M (tetrabutylammonium hydroxide) along with 0.4 mM of substrate in a methanol solvent. The reactions were monitored using a Cary 100 UV−visible spectrophotometer with the cell compartment thermostatted at 25.0 ± 0.1 °C. Second-order methoxide rate constants were evaluated from the gradients of the observed first-order rate constant (k_{obs}) v s[methoxide] plots. (The concentration of water at 0.02 M of tetrabutylammonium hydroxide in methanol was titrated (Karl Fisher) to be 46 ± 2 mM, and at 0.3 M it was found to be 480 ± 4 mM. Anhydrous methanol as received was found to contain 16 ± 1 mM of water.)

2.4. X-ray Diffraction. A crystal of **1**-Zn(II)$_2$:($^-$OH)($CF_3SO_3^-$)$_3$-($HOCH_3$) suitable for X-ray diffraction was grown from a methanol solution containing ligand **1**, Zn(CF_3SO_3)$_2$, and $NaOCH_3$ in a 1:2:1 ratio. The solution was allowed to evaporate exposed to the atmosphere at ambient temperature over 4 days. Structural details are given in Table 1 below and the ORTEP diagram for **1**:Zn$_2$:($^-$OH) at the 50% probability level is given in Figure 6. Full structural parameters and the CIF file are given in the Supporting Information.

3. Results

3.1. Methoxide-Promoted Reactions. In order to compare the catalysis afforded by **1**-Zn(II)$_2$:($^-$OCH$_3$) for cleavage of the substrates (**4**a−g) to the background reactions, the second-order rate constants for their methoxide-promoted cleavages were determined at 25 °C under pseudo-first-order conditions of excess [CH_3O^-] (0.02−0.3 M in methanol). In Table 2 are the second-order rate constants (k_2^{-OMe}) for each substrate along with the $^s_s pK_a$ values for the corresponding phenols in methanol. A Brønsted plot of the log k_2^{-OMe} vs $^s_s pK_a$ (not shown) fits a linear regression of log $k_2^{-OMe} = (-0.72 \pm 0.08)\ ^s_s pK_a + (5.36 \pm 1.08)$.

Table 1. Crystal Data and Structural Refinement Details for **1**-Zn(II)$_2$:($^-$OH)($CF_3SO_3^-$)$_3$($HOCH_3$)

empirical formula	$C_{25}H_{47}F_9N_6O_{11}S_3Zn_2$
formula weight	1005.61
temperature	180(2) K
wavelength	0.71073 Å
crystal system	monoclinic
space group	*P*2(1)/*c*
unit cell dimensions	$a = 10.9062(10)$ Å $b = 22.998(2)$ Å $c = 16.7888(14)$ Å $\alpha = 90°$ $\beta = 102.656(2)°$ $\gamma = 90°$
volume	4108.7(6) Å^3
Z	4
density (calculated)	1.626 Mg/m^3
absorption coefficient	1.419 mm^{-1}
F(000)	2064
crystal size	0.40 × 0.10 × 0.08 mm^3
θ range for data collection	1.53 to 25.00°.
index ranges	$-12 \le h \le 12$, $-27 \le k \le 27$, $-19 \le l \le 17$
reflections collected	23896
independent reflections	7225 [*R*(int) = 0.0303]
completeness to $\theta = 25.00°$	99.9%
absorption correction	empirical (Bruker SADABS)
max. and min. transmission	1.0000 and 0.8649
refinement method	full-matrix least-squares on F^2
data/restraints/parameters	7225/7/529
goodness-of-fit on f^2	1.000
final *R* indices [$I > 2\sigma(I)$]	R1 = 0.0373, wR2 = 0.0940
R indices (all data)	R1 = 0.0573, wR2 = 0.1005
largest diff. peak and hole	0.648 and −0.509 e·Å^{-3}

Table 2. Second-Order Rate Constants for the Methoxide Promoted Cleavage of **4**a−g, and $^s_s pK_a$ Values for the Corresponding Phenols in Methanol, $T = 25$ °C

substrate	phenol $^s_s pK_a$	k_2^{-OMe} (M^{-1}s^{-1})
4a **(2)**	11.30	$(2.6 \pm 0.2) \times 10^{-3}$[a]
4b	11.50	$(5.3 \pm 0.2) \times 10^{-4}$
4c	12.49	$(6.7 \pm 0.2) \times 10^{-4}$
4d	13.59	$(5.2 \pm 0.2) \times 10^{-5}$
4e	13.93	$(1.68 \pm 0.06) \times 10^{-5}$
4f	14.33	$(1.21 \pm 0.03) \times 10^{-5}$
4g	14.77	$(5.9 \pm 0.2) \times 10^{-6}$

[a] Rate constant from ref 9.

3.2. Cyclization Reaction of 4a−g Promoted by 1-Zn(II)$_2$:($^-$OCH$_3$) in Methanol. The plots of the k_{obs} for cyclization of **4**b, **4**c, and **4**f vs [**1**-Zn(II)$_2$:($^-$OCH$_3$)]$_{free}$ shown in Figures 1, 2, and 3 demonstrate progressive differences in passing from good aryloxy leaving groups to poorer ones with higher $^s_s pK_a$ values. Previously we have established that triflate ion is an inhibitor of the catalysis afforded by **1**:Zn(II)$_2$:($^-$OCH$_3$) with an inhibition constant of $K_i = 14.9$ mM[3a] from which one can determine the free catalyst concentration at any [triflate]. All the catalyst concentrations reported in the figures and used for computation of the kinetic parameters refer to the free concentrations corrected for triflate inhibition ([**1**-Zn(II)$_2$:($^-$OCH$_3$)]$_{free}$).

(14) Liu, T.; Neverov, A. A.; Tsang, J. S. W.; Brown, R. S. *Org. Biomol. Chem.* **2005**, *3*, 1525.

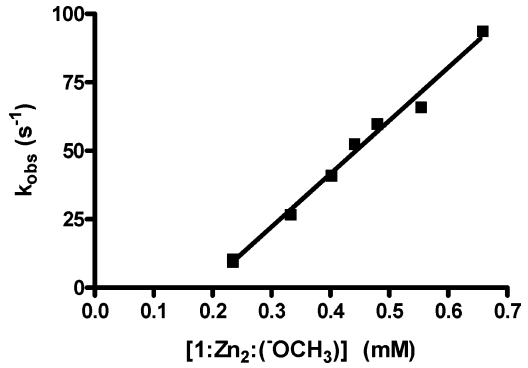

Figure 1. Plot of k_{obs} vs [**1**-Zn(II)$_2$:($^-$OCH$_3$)]$_{free}$ for the catalyzed methanolysis of **4**b (4×10^{-5} M) determined from the rate of appearance of product phenol at 323 nm, ^s_spH 9.8 ± 0.1, and 25.0 ± 0.1 °C. The linear regression gives $k_2^{obs} = (1.94 \pm 0.03) \times 10^5$ M^{-1} s^{-1} with an intercept of $A = 0.190 \pm 0.013$ mM.

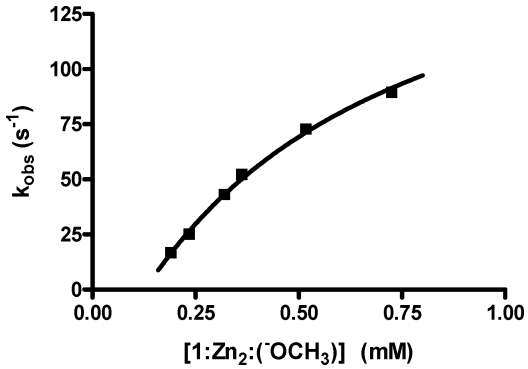

Figure 2. Plot of k_{obs} vs [**1**-Zn(II)$_2$:($^-$OCH$_3$)]$_{free}$ for the catalyzed methanolysis of **4**c (4×10^{-5} M) determined from the rate of appearance of product phenol at 340 nm, ^s_spH 9.8 ± 0.2, and 25.0 ± 0.1 °C. Fitting of the data to the expression given in eq 1 gives $K_M = (6.3 \pm 0.9) \times 10^{-4}$ M, $k_{cat}^{max} = 190 \pm 16$ s^{-1} and an intercept $A = 0.128 \pm 0.005$ mM.

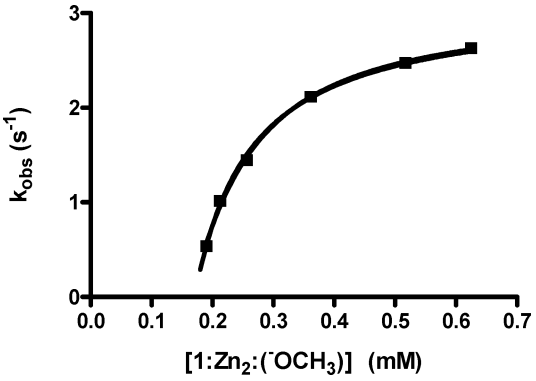

Figure 3. Plot of k_{obs} vs [**11**-Zn(II)$_2$:($^-$OCH$_3$)]$_{free}$ for the catalyzed methanolysis of **4**f (4×10^{-5}) M determined from the rate of appearance of phenol at 280 nm, ^s_spH 9.8 ± 0.1, and 25.0 ± 0.1 °C. Fitting of the data to the expression given in eq 1 gives $K_M = (1.00 \pm 0.08) \times 10^{-4}$ M, $k_{cat}^{max} = 3.10 \pm 0.06$ s^{-1} and intercept $A = 0.171 \pm 0.001$ mM.

Substrates **4**a and **4**b do not show saturation kinetics at the catalyst concentrations used, and the linear regressions of the respective plots give second-order rate constants for the appearance of phenol product of 275,000[3a] and 194,000 M^{-1} s^{-1}. The plot for substrate **4**c shows apparent saturation over the same range of [**1**-Zn(II)$_2$:($^-$OCH$_3$)]$_{free}$ from which nonlinear least-squares (NLLSQ) fitting of the data to the expression given in eq 1, vide infra, gives $K_M = (6.3 \pm 0.9) \times 10^{-4}$ M and $k_{cat}^{max} = 190 \pm 16$ s^{-1}. A more pronounced saturation is seen in Figure 3 for the less reactive **4**f, and fitting of these data to eq 1 gives $K_M = (1.00 \pm 0.08) \times 10^{-4}$ M and $k_{cat}^{max} = 3.10 \pm 0.06$ s^{-1}. Original data for all substrates and plots of k_{obs} vs [**1**-Zn(II)$_2$:($^-$OCH$_3$)]$_{free}$ are given as Supporting Information.

There are several points of note required to understand the fitted data. First, inspection of all the plots reveals that there is a significant *X*-intercept which results from incomplete formation of the catalyst at low concentrations. Equation 1 is a universal binding equation that is applicable to both strong and weak binding situations[15]

$$k_{obs} = k_{cat}(1 + K_B[S] + [Cat]K_B - X)/(2K_B)/[S] \quad (1)$$

where:

$$X = (1 + 2K_B[S] + 2[Cat]K_B + K_B^2[S]^2 - 2K_B^2[Cat][S] + [Cat]^2K_B^2)^{0.5}$$

and K_B refers to the Cat + Sub binding constant (units of M^{-1}), the reciprocal of which is defined here as the Michaelis−Menten constant K_M with units of M. The [Cat] term in eq 1 used for the fitting corresponds to the actual concentration of *viable* catalyst, free from triflate inhibition, which is derived according to the expression [Cat] = ([**1**:Zn(II)$_2$:($^-$OCH$_3$)]$_{free}$ − *A*), where *A* is an independently fitted parameter generally having the value around 0.2 mM, corresponding to the observable intercept. While we acknowledge this approach is not rigorous, it is the same as what we have used previously to model the La^{3+}-catalyzed methanolysis of carboxylate esters and neutral phosphate triesters[16a−c] where only the concentration of a catalytically active La^{3+}-containing dimer was taken into account. We have also demonstrated the validity of this approach in the case of the Zn^{2+}-catalyzed cyclization of HPNPP in ethanol.[4] Given in Table 3 are the best-fit K_M and k_{cat}^{max} constants for substrates **4**c−g, along with the experimentally observed second-order rate constants for substrates **4**a (or **2**[3a]) and **4**b. The k_{cat}^{max} values for substrates **4**a and **4**b were computed under the assumption that values for all the substrates adhere to a Brønsted relationship $k_{cat}^{max} = 10^{(\beta_{lg} \cdot {}^s_spK_a + C)}$. Nonlinear least-squares fitting of the available k_{cat}^{max} vs $^s_spK_a$ data gives $\beta_{lg} = -0.97 \pm 0.05$ and $C = 14.36 \pm 0.57$ from which values of 2300 ± 800 and 1470 ± 450 s^{-1} can be extrapolated for substrates **4**a and **4**b.[17] These are used to provide the K_M values from the expression $K_M = k_{cat}^{max}/k_2^{obs}$. Given in Figure 4 is a plot of the K_M vs phenol $^s_spK_a$ values that shows an upward curvature commencing at the more acidic phenols corresponding to substrates **4**c, **4**b, and **4**a. Also included on the figure are two complex constants, the components of which refer to various rate and equilibrium binding constants given in Scheme 1 which will be discussed later.

(15) Equation 1 was obtained from the equations for equilibrium binding and for conservation of mass by using the commercially available MAPLE software, *Maple 9.00*, June 13, 2003, Build ID 13164, Maplesoft, a division of Waterloo Maple Inc. 1981−2003, Waterloo, Ontario, Canada.

(16) (a) Brown, R. S.; Neverov, A. A.; Tsang, J. S. W.; Gibson, G. T. T.; Montoya-Peláez, P. J. *Can. J. Chem.* **2004**, *82*, 1791. (b) Brown, R. S.; Neverov, A. *J. Chem. Soc., Perkin Trans. 2* **2002**, 1039. (c) Tsang, J. S.; Neverov, A. A.; Brown, R. S. *J. Am. Chem. Soc.* **2003**, *125*, 7602.

(17) The linear regression of log k_{cat}^{max} vs $^s_spK_a$ fits the expression log $k_{cat}^{max} = (-0.89 \pm 0.13)$ $^s_spK_a + (13.20 \pm 1.78)$. Although the nonlinear and linear fittings give Brønsted β_{lg} values that are within experimental error, the nonlinear fit gives non-log-weighted error limits which reduce the uncertainty in the extrapolated k_{cat}^{max} terms for **4**a and **4**b.

Table 3. Kinetic Constants (Maximum Rate Constant, k_{cat}^{max}, Michaelis−Menten Constants (K_M), and Second-Order Rate Constants (k_2^{obs} or k_{cat}^{max}/K_M) for the Cleavage of **4**a−g Mediated by **1**-Zn(II)$_2$:($^-$OCH$_3$) at ^s_spH 9.8 and 25.0 ± 0.1 °C

substrate	phenol $^s_s pK_a$ in methanol	k_{cat}^{max} (s^{-1})	K_M (M)	k_2^{obs} ($M^{-1}\,s^{-1}$)	acceleration by catalyst at ^s_spH 9.8[c]
4a **(2)**[a]	11.30	*2300 ± 800*	*(8.3 ± 2.9) × 10^{-3}*	(2.75 ± 0.04) × 10^5	1.0 × 10^{12}[d]
4b[a]	11.50	*1470 ± 450*	*(7.2 ± 2.3) × 10^{-3}*	(1.94 ± 0.03) × 10^5	3.4 × 10^{12}[d]
4c	12.49	190 ± 16	(6.3 ± 0.9) × 10^{-4}	(3.0 ± 0.5) × 10^5[b]	2.6 × 10^{12}
4d	13.59	15.0 ± 0.4	(8.0 ± 0.8) × 10^{-5}	(1.9 ± 0.2) × 10^5[b]	2.7 × 10^{12}
4e	13.93	3.32 ± 0.09	(1.0 ± 0.1) × 10^{-4}	(2.6 ± 0.3) × 10^4[b]	1.8 × 10^{12}
4f	14.33	3.10 ± 0.07	(7.9 ± 0.8) × 10^{-5}	(3.9 ± 0.4) × 10^4[b]	2.4 × 10^{12}
4g	14.77	2.37 ± 0.07	(1.0 ± 0.1) × 10^{-4}	(2.3 ± 0.3) × 10^4[b]	3.8 × 10^{12}

[a] K_M values in italics computed as described in text. The k_2^{obs} values for **4**a[3a] and **4**b are the experimentally observed values from the slopes of the k_{obs} vs [**1**-Zn(II)$_2$:($^-$OCH$_3$))]$_{free}$ plots. [b] k_2^{obs} values computed from k_{cat}^{max}/K_M. [c] Acceleration in terms of k_{cat}^{max} relative to the methoxide reaction at ^s_spH 9.8 where [$^-$OCH$_3$] =1.07 × 10^{-7} M. [d] Acceleration in terms of 1 mM catalyst reacting with observed second-order rate constant at ^s_spH 9.8.

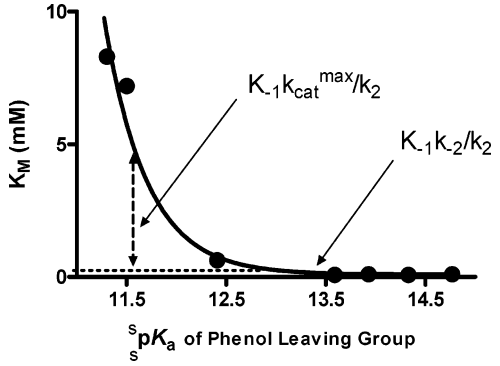

Figure 4. Plot of K_M vs $^s_s pK_a$ values for the phenols of substrates **4**a−g. K_M values for the substrates with the two lowest $^s_s pK_a$'s (**4**a,b) computed as described in text; K_M values for **4**c−g are experimentally determined from fits of the saturation kinetic plots. Line through the data computed on the basis of NLLSQ fit to $K_M = C + 10^{(\beta_{lg}\cdot{}^s_s pK_a + const.)}$ where β_{lg} has a computed value of −1.02 ± 0.13, constant is 12.5 ± 1.5 and $C = K_{-1}k_{-2}/k_2$ is set as a constant of 9 × 10^{-5} M (the average K_M value for substrates **4**d−g).

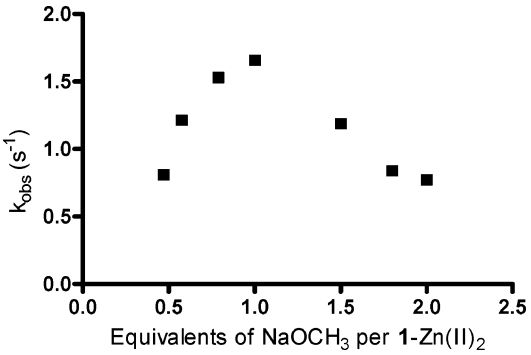

Figure 5. Plot of the observed first-order rate constants for the methanolysis of 0.04 mM **4**f catalyzed by 0.4 mM **1**-Zn(II)$_2$ as a function of the [CH_3O^-]/[**1**:Zn(II)$_2$] ratio at 25.0 ± 0.1 °C.

Shown in Figure 5 is a plot of the first-order rate constant for the appearance of phenol product from 4 × 10^{-5} M **4**f promoted by 0.4 mM **1**-Zn(II)$_2$ containing catalyst where the [methoxide]/[**1**-Zn(II)$_2$] ratio varies from 0 to 2. A 0.8 mM stock solution of the **1**-Zn(II)$_2$:($^-$OCH$_3$) catalyst was prepared as described in the Experimental Section and then mixed in a stopped-flow reaction analyzer with equal volumes of a second solution containing 0.08 mM of **4**f and varying amounts of added HClO$_4$ or NaOCH$_3$ after which the rate of appearance of product phenol was determined. As the figure shows, the maximum rate constant is observed when the [methoxide]/[**1**-Zn(II)$_2$] ratio is unity, consistent with a process where the TS

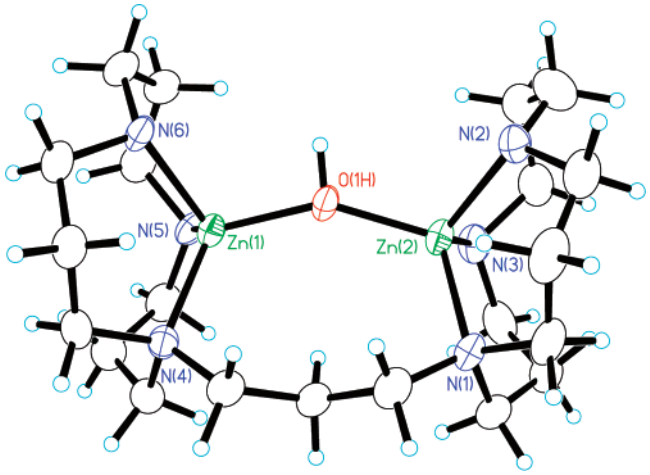

Figure 6. Molecular structure of **1**-Zn(II)$_2$:($^-$OH) ($CF_3SO_3^-$)$_3$(HOCH$_3$) shown as an ORTEP diagram at the 50% probability level, counterions and methanol of solvation omitted for clarity. Structural details given in Supporting Information.

for the product appearance contains one methoxide, one **1**-Zn-(II)$_2$ complex, and one substrate, or their kinetic equivalents.

A crystal of **1**-Zn(II)$_2$:($^-$OH) ($CF_3SO_3^-$)$_3$(HOCH$_3$) suitable for X-ray diffraction was grown from a methanol solution where the components **1**, Zn($CF_3SO_3^-$)$_2$, and NaOCH$_3$ were introduced in a 1:2:1 ratio. Surprisingly, the structure of the core unit shown in Figure 6 (devoid of the three triflate counterions and the methanol of solvation) shows a hydroxide ion bridging between the two Zn(II) ions, the source of which must be adventitious water that was present in the methanol solution or in the atmosphere to which the solution was exposed during its evaporation.

4. Discussion

4.1. X-ray Diffraction Structure. Despite having been grown from a methanol solution with added methoxide, the only crystallized complex we obtained contains a bridging hydroxide as **1**-Zn(II)$_2$:($^-$OH). Its molecular structure, shown in Figure 6 devoid of counterions and methanol of solvation, shows that each metal ion is coordinated to a single bridging HO$^-$ and the three N's of the opposing triazacyclododecane units that are joined by a 1,3-propano linker in a fashion that is reminiscent of "earmuffs". The Zn(II)$_2$-coordinated hydroxide is hydrogen bonded to a triflate ion in the adjacent unit cell which may be a stabilizing force for HO$^-$ in the solid state, although it is possible that there is some other subtle preference for hydroxide that is retained in solution, but this cannot be ascertained from

the studies we have at present. Each of the Zn(II) ions experiences a distorted tetrahedral coordination with the HO$^-$−Zn−N angles varying between 105° and 117°. The Zn−$^-$OH bond lengths are 1.912(2) and 1.915(2) Å, while the Zn−$^-$O-(H)−Zn angle is 147.19(14)°. The Zn−Zn separation is 3.670 Å which can be compared with Cu(II)−Cu(II) separations of 3.26 and 3.68 Å in two related **1**-Cu(II)$_2$:($^-$OH)(OH$_2$) and **1**-Cu-(II)$_2$:($^-$OH)((ArCH$_2$O)$_2$PO$_2^-$) complexes previously reported.[3b] We have repeatedly tried, without success, to obtain a dibenzyl phosphate complex of **1**-Zn(II)$_2$:($^-$OH), but the only crystalline products are those containing polymeric $Zn^{2+}{}_2$((ArCH$_2$O)$_2$PO$_2^-$)$_2$ with no ligand present.

4.2. Methoxide-Promoted Cyclization of 4a−g. The Brønsted plot of the log $k_2{}^{-OMe}$ vs phenol $^{s}_{s}pK_a$ data (Table 2) has a β_{lg} value of −0.72 ± 0.08. This value can be compared with β_{lg} values of −0.62 and −0.58 for the hydroxide-promoted cleavage of 2-hydroxypropyl aryl phosphates and for the hydroxide-promoted hydrolysis of methyl aryl phosphate diesters[18] and values of −0.54 for the hydroxide reaction of aryl uridine-3′-phosphates,[19a] and −0.64 for the attack of aryloxy anions on aryl methyl phosphate diesters.[19b] Williams[19,20] has argued that nucleophilic displacement of good leaving groups from neutral or monoanionic phosphates by oxyanions is concerted or involves an intermediate in a very shallow energy well at the top of a barrier. The more recent study[21] indicated the base-catalyzed ring closure of a series of uridine 3′-phosphate esters with leaving groups spanning a range of 5−17 pK_a units proceeded through an intermediate, the formation and breakdown of which was rate limiting for good and poor leaving groups respectively (β_{lg} = −0.52 and −1.34, respectively). In the latter report[21] it was argued that the original Brown and Usher data for the base-promoted cyclization of 2-hydroxypropyl aryloxy and alkoxy phosphates[10] could be reasonably reinterpreted as being consistent with a stepwise process proceeding through a five-membered phosphorane intermediate.

The data we have with the methoxide reaction of **4**a−g are consistent with a single rate-limiting step for these substrates having a limited $^{s}_{s}pK_a$ range for the various aryloxy-leaving groups. This includes a two-step process where formation of the phosphorane intermediate is rate limiting with fast loss of the good leaving groups. At the transition state, the change in bonding of ArO−P bond has progressed some 40−45% from starting material to product phenolate.[22] The observed reaction with substrates **4** in both water and methanol does not incorporate lyoxide, but rather involves specific base-promoted cyclization with the expulsion of the substituted phenoxide (which immediately produces phenol at these $^{s}_{s}$pH values in methanol) as in eq 2. The methanol solvent actually reduces the base-catalyzed reaction rates relative to the situation in water. For example with **4**a, the $k_2{}^{-OMe}$ is 2.6 × 10^{-3} M^{-1} s^{-1}, [9] while that for the hydroxide-promoted cyclization is reported as 9.9 × 10^{-2} M^{-1} s^{-1} [23] or 6.5 × 10^{-2} M^{-1} s^{-1}.[24]

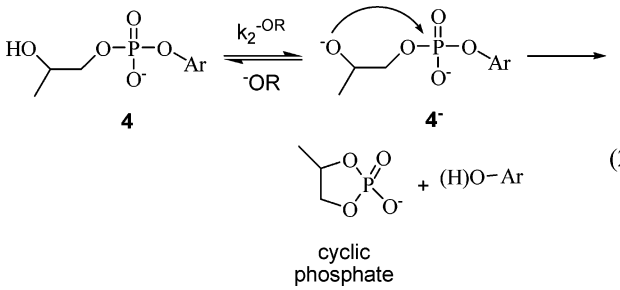

(2)

This rate reduction is probably a consequence of the reduced polarity/dielectric constant of methanol vs water (ϵ = 31.5 vs 78[25]) which opposes the required pre-equilibrium formation of the dianionic form (**4**$^-$). Nevertheless, as will be shown later, this same reduced dielectric constant/polarity effect considerably enhances the reactions between the substrates **4** and the net positively charged **1**-Zn(II)$_2$:($^-$OCH$_3$) catalyst.

4.3. Cyclization Reactions of 4a−g Catalyzed by 1-Zn-(II)$_2$:($^-$OCH$_3$). 4.3.1. Stepwise or Concerted k_{cat} Process? Inspection of the k_{obs} vs [**1**-Zn(II)$_2$:($^-$OCH$_3$)]$_{free}$ plots provided in Figures 1−3 for **4**b,c,f, as well as those figures in the Supporting Information for **4**d,e,g, indicates that all substrates but **4**a[3a] and **4**b exhibit Michaelis−Menten behavior over the range of 0.2 mM < [**1**-Zn(II)$_2$:($^-$OCH$_3$)]$_{free}$ < 1 mM. The K_M and $k_{cat}{}^{max}$ constants in Table 3 for **4**c−g are derived from fitting the k_{obs} vs [**1**-Zn(II)$_2$:($^-$OCH$_3$)]$_{free}$ data to the expression in eq 1. Since the k_{obs} plots for **4**a,b are linear over the concentration range investigated, only second-order rate constants for the appearance of the corresponding phenol products are experimentally accessible. However, under the assumption that the $k_{cat}{}^{max}$ for **4**a and **4**b should lie on the same Brønsted plot that is defined by the other members of series **4**, respective values of 2300 and 1470 s^{-1} can be determined for these. This assumption might be questioned since it requires that the mechanism for the $k_{cat}{}^{max}$ term involving cleavage of the bound phosphate should be a common one throughout this series of closely related aryloxy derivatives. In our opinion it is likely that the present **1**-Zn(II)$_2$:($^-$OCH$_3$)-catalyzed cyclization reactions of **4**a−g all comprise two steps since the strong electrostatic interaction of the dinuclear core of the catalyst should stabilize greatly the dianionic phosphorane intermediate and the transition state leading to it, thereby deflecting the reaction away from a concerted pathway. Since we are dealing with good aryloxy-leaving groups, the probable rate-limiting step is the formation of the intermediate, but the slightly more negative Brønsted β_{lg} value for the catalyzed k_{cat} reaction (−0.97 ± 0.05) relative to that of the second-order methoxide-promoted reaction (−0.72 ± 0.08) weakly suggests that there is more P−OAr bond cleavage at the TS in the former.

(18) Williams, N. H.; Takasaki, B.; Wall, M.; Chin, J. *Acc. Chem. Res.* **1999**, *32*, 485.
(19) (a) Davis, A. M.; Hall, A. D.; Williams, A. *J. Am. Chem. Soc.* **1998**, *110*, 5105. (b) Ba-Saif, S. A.; Davis, A. M.; Williams, A. *J. Org. Chem.* **1989**, *54*, 5483.
(20) (a) Bourne, N.; Williams, A. *J. Am. Chem. Soc.* **1984**, *106*, 7591. (b) Bourne, N.; Chrystiuk, E.; Davis, A. M.; Williams, A. *J. Am. Chem. Soc.* **1988**, *110*, 1890.
(21) Lönnberg, H.; Strömberg, R.; Williams, A. *Org. Biomol. Chem.* **2004**, *2*, 2165.
(22) The extent of breaking of the P−OAr bond in the TS can be measured by the Leffler parameter, *a*, which measures the change in the Brønsted β_{lg} for the TS relative to the b_{eq} for equilibrium transfers of the phosphoryl group between oxyanion nucleophiles. In the case of the transfer of the (RO)P(=O)O$^-$ group[20a], the β_{eq} value is −1.74 with the *O*−Ar oxygen in the starting material having a net effective charge of +0.74. When methoxide is the nucleophile, the Leffler parameter of β_{lg}/β_{eq} = 0.43 suggests that the P−OAr cleavage is 43% of the way from starting material to product.
(23) O'Donoghue, A. M.; Pyun, S. Y; Yang, M.-Y.; Morrow, J. R.; Richard, J. P. *J. Am. Chem. Soc.* **2006**, *128*, 1615.
(24) Bonfá, L.; Gatos, M.; Mancin, F.; Tecilla, P.; Tonellato, U. *Inorg. Chem.* **2003**, *42*, 3943.
(25) Harned, H. S.; Owen, B. B. *The Physical Chemistry of Electrolytic Solutions*, 3rd ed.; ACS Monograph Series 137; Reinhold Publishing: New York, 1957; p 161.

4.3.2. Break in the K_M vs ${}^{s}_{s}pK_a$ Plot. From the extrapolated k_{cat}^{max} values for **4**a and **4**b can be derived K_M constants of 8.3×10^{-3} and 7.2×10^{-3} M respectively, with errors of about ±30%. All the K_M values are plotted in Figure 4 against the phenol ${}^{s}_{s}pK_a$ values and NLLSQ fitting of the data to $K_M = C + 10^{(\beta_{lg} \cdot {}^{s}_{s}pK_a + \text{const.})}$ provides a β_{lg} value of -1.02 ± 0.13. This value is largely defined by the k_{cat}^{max} term which starts to come into play for the substrates where the leaving phenols have ${}^{s}_{s}pK_a$ values of less than ~13.

The Michaelis−Menten expression given in eq 3 can be derived for the process given in Scheme 1,

$$\text{rate} = \frac{dP}{dt} = \frac{k_{cat}^{max}[\mathbf{1} - \text{Zn(II)}_2{:}(^{-}\text{OCH}_3)]_{free}[4]}{K_M + [\mathbf{4}]} \quad (3)$$

$$K_M = \frac{k_{-1}}{k_1} \bullet \frac{k_{-2} + k_{cat}^{max}}{k_2} = K_{-1}\frac{k_{-2}}{k_2} + K_{-1}\frac{k_{cat}^{max}}{k_2} \quad (4)$$

with the K_M constant being defined in eq 4. In our model, the k_{-1}/k_1 term refers to an equilibrium dissociation constant of a first-formed complex where the substrate is bound to one of the Zn(II) ions (herein termed K_{-1} for simplicity). The k_2 term refers to a subsequent step proposed to be an intramolecular rearrangement where the substrate becomes bound to both of the Zn(II) ions, experiencing a double activation as shown in Scheme 1, and the k_{cat}^{max} term corresponds to the chemical step of intramolecular cyclization which produces the observed phenol product. We note that it is not mathematically required that we include the first equilibrium constant k_{-1}/k_1 or K_{-1} in the analysis but suggest it is necessary for a more complete description based on two considerations. First, it is difficult to envision that a productive substrate association involving phosphate coordination to both metal ions can occur in a single step with the highly congested **1**-Zn(II)$_2$:($^{-}$OCH$_3$) as it would involve formation of two P−O−Zn(II) bonds along with the cleavage of at least one Zn(II)−$^{-}$OCH$_3$ linkage in a very sterically restricted complex. This explains the rather small, second-order rate constants of 275,000 and 194,000 M^{-1} s^{-1} observed for catalyzed reactions of **4**a and **4**b[26] that seem low for a binding event involving a facile ligand exchange on Zn(II) which, in favorable cases, can be as high as 10^7-10^8 M^{-1} s^{-1}.[27] The rates of binding to M(II) complexes in general are known[28] to be highly sensitive to crowding effects such as is expected with **1**-Zn(II)$_2$:($^{-}$OCH$_3$) (see structure in Figure 6). Second, for the analogous **1**-Cu(II)$_2$:($^{-}$OCH$_3$) complex, stopped-flow spectrophotometry reveals that the kinetics of changes of the Cu(II) absorbance bands in the presence of some phosphate substrates including **4**a and **3** are consistent with two events; a bimolecular binding of substrate and **1**-Cu(II)$_2$:($^{-}$OCH$_3$) followed by a unimolecular rearrangement of what appears to be a first-formed complex that evolves into reactive form where we suggest that the phosphate is doubly coordinated by the Cu(II)$_2$ moiety.[3b]

Among all the terms present in Scheme 1, the k_{cat}^{max} constant should be most sensitive to the nature of the aryloxy group, and the binding terms K_{-1}, k_2, and k_{-2} are expected to be much less so. For the analysis, these will be assumed to be invariant constants for the series **4** substrates. The form of eq 4 breaks the K_M term into two components, the first of which ($K_{-1}k_{-2}/k_2$) should be insensitive to the nature of the leaving group, and thus largely defines the K_M values for the poorer substrates. Accordingly, for substrates **4**d−g, all the experimental K_M values are very close, lying in the range of 8×10^{-5} M to 1×10^{-4} M, and this is shown graphically in Figure 4 as a dotted horizontal line. For the substrates with the better leaving groups, the second term in eq 4, $K_{-1}k_{cat}^{max}/k_2$, comes into play, causing increases in the K_M to 6.3×10^{-4} M for **4**c and calculated values of 7.2×10^{-3} and 8.3×10^{-3} M for **4**b and **4**a as a result of an increasing k_{cat}^{max} (190 to 1470 and then 2300 s^{-1} respectively). The upward curvature seen in Figure 4 largely depends on how the electronic changes in the substrate affects the ratio of ($k_{-2} + k_{cat}^{max}$)/k_2 and provides evidence for a change in the rate-limiting step from chemical cleavage for poor substrates (leaving-group ${}^{s}_{s}pK_a$ values are >13) to binding for good substrates (leaving-group ${}^{s}_{s}pK_a$ values are <12.5) for which $k_{cat}^{max} > k_{-2}$.

Some information about the values of the complex constants comes from analysis of the relationship given in Figure 4 where the average K_M for substrates **4**d−g is 9×10^{-5} M and is equal to $K_{-1}k_{-2}/k_2$ in Scheme 1. This number is very close to the observed inhibition constant of 1.6×10^{-4} M for the essentially unreactive, but structurally analogous, complex of dibenzyl phosphate and **1**-Zn(II)$_2$:($^{-}$OCH$_3$).[3a] Using the experimentally determined K_M and k_{cat}^{max} values of 6.3×10^{-4} M and 190 s^{-1} for **4**c (Table 3), one calculates from eq 4 values of 32 s^{-1} for k_{-2} and 2.84×10^{-6} M·s for the ratio K_{-1}/k_2 or its reciprocal of 352,000 M^{-1} s^{-1} for k_1k_2/k_{-1}. This latter number is the computed second-order rate constant for the binding of substrate to form the Michaelis complex, and can be compared with the experimental values of 275,000 and 194,000 M^{-1} s^{-1} found for substrates **4**a and **4**b[26]. Given the assumptions, the closeness of the computed and experimental numbers for a substrate, where saturation kinetics are observed, and two others, where only second-order kinetics are observed, gives support for the qualitative correctness of the proposed change in the rate-limiting step from chemical cleavage to substrate binding as we progress from poor to good substrates.

4.4. Catalysis and Mechanistic Questions. Presented in Scheme 2 is a more detailed version of Scheme 1 that gives the possible candidates involved in the **1**-Zn(II)$_2$:($^{-}$OCH$_3$)-catalyzed cleavage of substrates **4**. Inspection of Figure 5 indicates that for substrate **4**f where Michaelis−Menten kinetics are observed and the concentration of catalyst is great enough that the Michaelis complex is essentially completely formed, the k_{cat} rate constant for production of product maximizes at 1 equiv of methoxide per **1**:Zn(II)$_2$ unit. This stopped-flow experiment is conducted starting with the fully formed **1**-Zn(II)$_2$:($^{-}$OCH$_3$) catalyst which is mixed rapidly with **4**f and an appropriate amount of $HClO_4$ or $Bu_4N^{+}(^{-}OCH_3)$. Under the assumptions that the substrate binding and acid/base reactions

(26) According to our proposed mechanism, the chemical step for catalyzed cleavage of **4**a and **4**b is not rate limiting, but the binding steps are. Steady-state analysis of the binding with k_2 being rate limiting gives $k_{obs} = k_1k_2/(k_{-1} + k_2)$.

(27) Another possibility for the rather slow binding of the substrate to the catalyst could be an unfavourable pre-equilibrium opening of one of the Zn(II)−OCH$_3$ linkages, followed by a rapid attack of the substrate, which then undergoes double activation and subsequent reaction. This process is kinetically equivalent to what we have proposed.

(28) (a) Dukes, G. R.; Margerum, D. W. *Inorg. Chem.* **1972**, *11*, 2952. (b) Pitteri, B.; Marangoni, G.; Viseutin, F. V.; Cattalini, L.; Bobbo, T. *Polyhedron* **1998**, *17*, 475.

Scheme 2. Simplified Proposed Scheme for Binding and Catalyzed Cyclization of 2-Hydroxypropyl Aryl Phosphates Promoted by **1**:Zn_2:($^-OCH_3$)

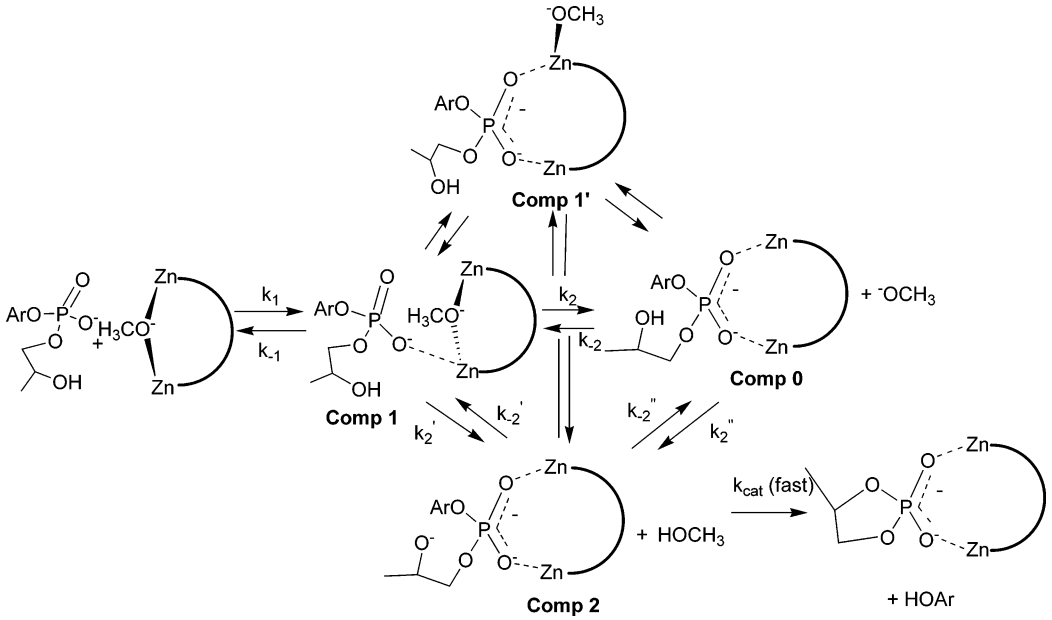

Scheme 3

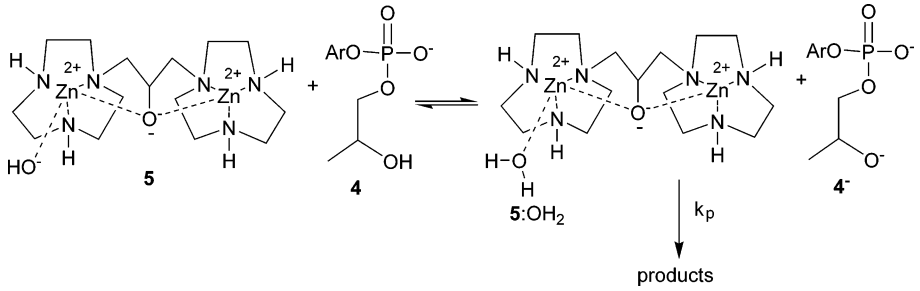

are fast and the metal ion does not dissociate from the complex within this time scale, the results suggest that the TS for the catalytic formation of the phenol product contains one each of methoxide, substrate, and **1**-Zn(II)$_2$, or the kinetic equivalent. Substrate **4**a exhibits a linear dependence on [catalyst] for the production of *p*-nitrophenol product and shows a quite different dependence for the plot of k_{obs}vs the [$^-OCH_3$]/[**1**:Zn(II)$_2$] ratio. This plot maximizes at ~0.1−0.2 at which point the k_{obs} is about 1.6-fold larger than when the[$^-OCH_3$]/[**1**:Zn_2] ratio is unity, and falls dramatically at lower ratios. This is consistent with a rate-limiting step where there is preferential **4**a binding to a **1**-Zn-(II)$_2$ complex without an associated methoxide. The drop in rate at [$^-OCH_3$]/[**1**-Zn(II)$_2$] ratio of ~0.1−0.2 is then consistent with a reduction in the free [$^-OCH_3$] to the point that the production of the product, which requires a deprotonation of the bound substrate, now becomes rate limiting.

There are two other aspects for which information is now available to rule out some of the mechanistic alternatives. The first is the state of ionization of the catalyst and substrate for the binding steps. It has been suggested,[8,23] on the basis of studies of the cleavages of some RNA models including uridine 3′-*p*-nitrophenyl phosphate and **4**a by the dinuclear Zn(II)catalyst **5** and some other metal ion-containing catalysts,[29,30] that the actual substrate-binding step may involve the deprotonated 2-OH form of the substrate (**4**$^-$) and the protonated form of the catalyst (**5**-Zn(II)$_2$:(OH_2)), rather than the alternative 2-OH form of the substrate with the deprotonated form of the catalyst (see Scheme 3). While this mechanism cannot be ruled out in general for the processes in water, it can be excluded for **1**-Zn(II)$_2$:($^-OCH_3$) in methanol. The pK_a for deprotonation of the 2-HO group of anionic **4**a in methanol should be at least as large or greater than that of methanol (K_w/[MeOH] = ($10^{-16.77}$/30)M) or ^s_spK_a ≥ 18.2. At a ^s_spH of 9.8 where the **1**-Zn(II)$_2$ catalyst is operative, the dianionic [**4**$^-$] would be one part in $10^{8.4}$. Since the second-order rate constants for binding of substrates **4**a and **4**b, in whatever form, by the **1**-Zn(II)$_2$ catalyst are observed to be 275,000 and 194,000 M^{-1} s^{-1} respectively, these reactions would have to exceed the diffusion limit of 10^{10} M^{-1} s^{-1} by at least 10^4 if the dianionic form of the substrate was the requisite form for binding. This factor must be even larger if one acknowledges that at ^s_spH 9.8 essentially all of the catalyst is present as **1**-Zn(II)$_2$:($^-OCH_3$) and only a small proportion exists in the form required to bind the anionic substrate, namely **1**-Zn-(II)$_2$:($HOCH_3$). Note this does not preclude a kinetically equivalent situation where there is transient binding of **1**:Zn-(II)$_2$:($^-OCH_3$) and **4** with a subsequent fast formation of a bound **1**:Zn(II)$_2$:**4**$^-$ form along with simultaneous or subsequent double activation and cyclization.

(29) Farquhar, E. R.; Richard, J. P.; Morrow, J. R. *Inorg. Chem.* **2007**, *46*, 7169.
(30) Mathews, R. A.; Rossiter, C. S.; Morrow, J. R.; Richard, J. R. *Dalton Trans.* **2007**, 3804.

Our favored mechanism shown in Scheme 2 thus involves the binding of **1**-Zn(II)$_2$:($^-$OCH$_3$) to the aryloxy hydroxypropyl phosphate (**4**) first through one of the metal ions, followed by a rearrangement to doubly activate the phosphate[31] via binding to the second Zn(II) ion. In accordance with the X-ray structure shown in Figure 6, we believe the resting state of **1**:Zn$_2$:($^-$OCH$_3$) in solution has the methoxy group bridging the two Zn(II) ions. In Scheme 2 the first formed complex (**Comp 1**) is formulated as having the phosphate bound to one of the Zn(II) ions so that its binding to the bridging methoxy group is loosened or lost completely. The process by which the double activation occurs is not clear from the present data, but could involve: (1) phosphate closure on the second Zn(II) to yield **Comp 1′** which retains the methoxy coordinated to the second Zn(II); (2) complete loss of the methoxide during the phosphate closure to give **Comp 0** plus liberated methoxide; or (3) formation of **Comp 2** where the departing methoxide has removed the 2-OH proton of the bound substrate during the process of double activation. If this process is reversible, it is equivalent to specific base removal of the 2-OH proton by an external methoxide followed by subsequent ring closure. The available kinetic evidence indicates the specific base role for external methoxide is possible, but only if deprotonation occurs at rates approaching the diffusion limit. For the fastest substrate where Michaelis−Menten behavior is observed in the concentration range investigated here (**4**c), the experimental k_{cat} value for the completely bound substrate is 190 s^{-1}. Assuming that external methoxide is the base, its concentration at $^{s}_{s}$pH 9.8 would be 1 × 10^{-7} M. Thus, if proton removal occurs at the diffusion limit of ∼10^{10} M^{-1} s^{-1}, the k_{cat} would have an upper limit ∼1000 s^{-1} which encompasses the observed value for **4**c, and those values predicted for **4**a and **4**b.

4.5. Catalytic Acceleration of the Cyclization of 4 and Energetic Considerations. Presented in Table 3 are accelerations provided by **1**-Zn(II)$_2$:($^-$OCH$_3$) for the cyclization reaction of **4**a−g relative to the rates contributed by the methoxide reactions (Table 2) at $^{s}_{s}$pH 9.8. Interestingly, all accelerations lie in the range of 1 − 4 × 10^{12}-fold. An alternative assessment compares the second-order rate constants for reaction of **1**-Zn(II)$_2$:($^-$OCH$_3$) with **4**a−g (defined as k_{cat}/K_M) with the k_2^{-OMe} values for the methoxide reactions (Table 2). These fit into a domain of (1−4.5) × 10^8-fold acceleration for **4**a−d, and a second domain of (1.5−4) × 10^9-fold for the less reactive substrates **4**e−g.

A convenient way[23] to quantify the catalytic efficiency is to calculate the difference in energy of a transition state containing only [CH$_3$O$^-$:**4**], and one where the latter is bound to the catalyst[32] (**1**-Zn(II)$_2$) to form a hypothetical transition state [**1**-Zn(II)$_2$:($^-$OCH$_3$):**4**]‡. Presented in Scheme 4 is a thermodynamic cycle involving both the methoxide reaction and the **1**-Zn(II)$_2$:($^-$OCH$_3$)-promoted (or kinetically equivalent) reactions of **4**c−g, for which eq 5 provides the free energy difference ($\Delta\Delta G^‡_{stab.}$) between [**1**:Zn(II)$_2$:($^-$OCH$_3$):**4**]‡ relative to [CH$_3$O$^-$:**4**]‡. In Scheme 4, $\Delta G_{bind,}$ $\Delta G^‡_{cat}$ and $\Delta G^‡_{Non}$ are the respective free energies for: (1) methoxide binding to **1**-Zn(II)$_2$, (2) the free energy of activation for unimolecular reaction of the **1**-Zn(II)$_2$:($^-$OCH$_3$):**4** complex or its kinetic equivalent, and (3) the free energy of activation for the reaction of methoxide with **4**. ΔG_M is the free energy for association of **4** and **1**-Zn(II)$_2$:($^-$OCH$_3$) computed from the Michaelis constant K_M for each substrate. In eq 6 the free energy calculation is specific for the reactions with **4**a,b that show only a first-order dependence on [**1**-Zn(II)$_2$:($^-$OCH$_3$)]$_{free}$ throughout the concentration range investigated.

Scheme 4

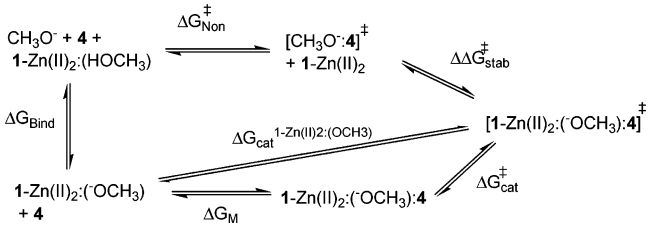

$$\Delta\Delta G^‡_{stab} = (\Delta G_{Bind} - \Delta G_M + \Delta G^‡_{cat}) - \Delta G^‡_{Non} = -RT\ln\left[\frac{(k_{cat}/K_M)(K_a/K_w)}{k_2^{-OMe}}\right] \quad (5)$$

$$\Delta\Delta G^‡_{stab} = (\Delta G_{Bind} + \Delta G_{cat}^{\mathbf{1}:Zn(II)2:(OCH3)}) - \Delta G^‡_{Non} = -RT\ln\left[\frac{(k_2^{obs})(K_a/K_w)}{k_2^{-OMe}}\right] \quad (6)$$

The various terms in eqs 5,6 are: (1) the k_{cat}/K_M values given in Table 3. The observed second-order rate constant (k_2^{obs}) for the reaction of **1**-Zn(II)$_2$:($^-$OCH$_3$) with **4**a,b is equivalent to this and is also found in Table 3; (2) K_a/K_w which can be readily shown to be formally equivalent to the binding constant of methoxide to the dinuclear complex **1**-Zn(II)$_2$ to form **1**-Zn(II)$_2$:($^-$OCH$_3$). K_a refers to the first acid dissociation constant of **1**-Zn(II)$_2$:(HOCH$_3$), determined from half-neutralization[3b] as 10$^{-9.41}$, and K_w is the autoprotolysis constant for methanol (10$^{-16.77}$); and (3) k_2^{-OMe} is the second-order rate constant for the methoxide reaction of each substrate given in Table 2.

Listed in Table 4 are the $(k_{cat}/K_M)/k_2^{-OMe}$and $(k_{cat}/K_M)(K_a/K_w)$ constants and computed $\Delta\Delta G^‡_{stab}$ values which are −21 to −23 kcal/mol. The first ratio provides the acceleration in second-order rate constant for the complex-catalyzed reaction relative to the methoxide reaction, while the second, when inserted into eqs 5,6, provides the free energy of stabilization ($\Delta\Delta G^‡_{stab}$) of the complex-catalyzed reaction relative to the methoxide reaction. Of these constants, the K_a/K_w term contributes −10.0 kcal/mol to the $\Delta\Delta G^‡_{stab}$ for the series, and the $(k_{cat}/K_M)/k_2^{-OMe}$ term contributes −11.0 to −13.2 kcal/mol with the slowest-reacting substrates having the more negative values.

It instructive to look at the graphical representation of the activation energy diagram shown in Figure 7 for the reaction of one example of the substrates, **4**c, with methoxide and the catalyst (represented as **1**:Zn(II)$_2$:($^-$OCH$_3$)),[33] all species at a standard state of 1 M, where the ground state comprises CH$_3$O$^-$, **1**-Zn(II)$_2$, and substrate **4**c partners. The $\Delta G^‡_{non}$ for the methoxide reaction in the absence of catalyst is 21.7 kcal/mol above the ground state. Figure 7 shows that binding of the three components to form the Michaelis complex, formulated as **1**:Zn(II)$_2$:($^-$OCH$_3$):**4**c, is exothermic by −14.4 kcal/mol, which is almost exactly offset by the activation energy of 14.3 kcal/mol

(31) Double Lewis, activation of phosphates is a well-known motif of the binding of a phosphate mono or dianion to a dinuclear core. See refs 1, 7, 8, 18, and Kinoshita, E.; Takahashi, M.; Takada, H.; Shiro, M. Koike, T. *Dalton Trans.* **2004**, *8*, 1189.
(32) Wolfenden, R. *Nature* **1969**, *223*, 704.

Table 4. $(k_{cat}/K_M)(K_a/K_w)$ and $(k_{cat}/K_M)/k_2^{-OMe}$ Constants and Computed Free Energies of Formation of Michaelis Complex ($\Delta G_{Bind} - \Delta G_M$), the Free Energies of Activation for k_{cat} ($\Delta G^{\ddagger}_{cat}$), and the Free Energies of Stabilization of the Methoxide Transition State through Binding to **1**-Zn(II)$_2$ ($\Delta\Delta G^{\ddagger}_{stab}$)[a] for the Reaction of **1**-Zn(II)$_2$:($^-$OCH$_3$) with Substrates **4**a−g at 25 °C in Methanol

substrate	$(k_{cat}/K_M)/k_2^{-OMe}$	$(k_{cat}/K_M)(K_a/K_w)$ ($M^{-2}\,s^{-1}$)[b,c]	$\Delta G_{Bind} - \Delta G_M$ (kcal/mol)[d]	$\Delta G^{\ddagger}_{cat}$ (kcal/mol)[e]	$\Delta\Delta G^{\ddagger}_{stab}$ (kcal/mol)
4a	1.15×10^8	6.3×10^{12}	−12.9	12.8	−21.0
4b	3.7×10^8	4.5×10^{12}	−13.0	13.1	−21.7
4c	4.5×10^8	6.9×10^{12}	−14.4	14.3	−21.8
4d	3.6×10^9	4.4×10^{12}	−15.6	15.8	−23.1
4e	1.5×10^9	6.0×10^{11}	−15.5	16.7	−22.6
4f	3.2×10^9	9.0×10^{11}	−15.6	16.8	−23.0
4g	3.9×10^9	5.3×10^{11}	−15.5	16.9	−23.1

[a] $\Delta G^{\ddagger}_{stab}$ computed from application of kinetic and equilibrium constants to eqs 5, 6; k_2^{-OMe} constants from Table 2. [b] k_{cat}/K_M from Table 3 [c] K_a determined from half-neutralization[3b] to be $10^{-9.41}$; $K_w = 10^{-16.77}$; $K_a/K_w = 2.3 \times 10^7$. [d] Computed as $(\Delta G_{Bind} - \Delta G_M) = -RT \ln((K_a/K_w)/K_M)$. [e] Computed from $\Delta G^{\ddagger}_{cat} = -RT \ln(k_{cat}/(kT/h))$ from the Eyring equation where $(kT/h) = 6 \times 10^{12}\ s^{-1}$ at 298 K.

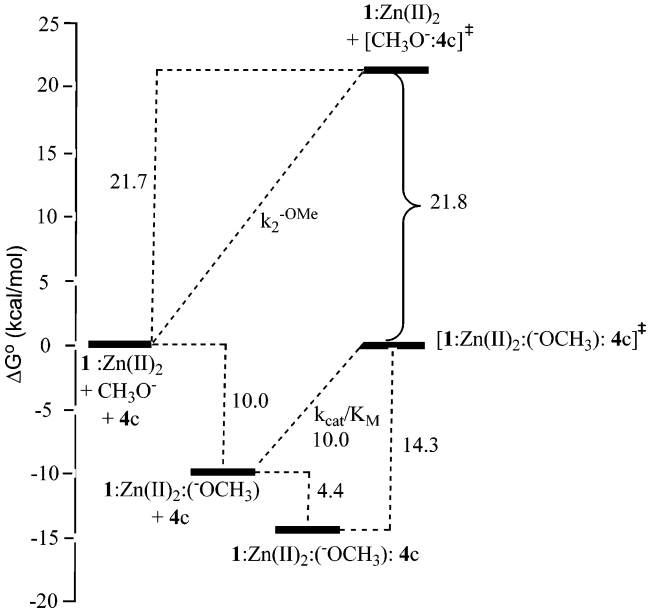

Figure 7. Activation energy diagram for the reaction of CH_3O^- and **1**:Zn(II):($^-$OCH$_3$) with substrate **4c** at standard state of 1 M and $T = 25$ °C showing the calculated energies of binding the methoxide by **1**:Zn(II)$_2$, of binding of the substrate to **1**:Zn(II)$_2$:($^-$OCH$_3$), and the calculated activation energies associated with k_{cat} and k_2^{-OMe}.

associated with the k_{cat}^{max} term.[34] Even for the substrates that do not show saturation kinetics (**4**a,b), the diagram shows that the computed energy of activation for the second-order rate constant for reaction of **4**a,b with **1**:Zn(II)$_2$:($^-$OCH$_3$) is 10.0 and 10.2 kcal/mol, respectively, again essentially offsetting exactly the energy of binding of methoxide to **1**:Zn(II)$_2$. It seems an important consequence that the catalyzed process of cyclization of the good substrates is energy neutral in passing from the ground state to the transition state of the activated complex, and that the overall rate of the reaction should be controlled by the rate of association of the components.

As presented in column 4 of Table 4, the catalyzed cyclization of all substrates **4** involves an assembly of the essential components (**1**-Zn(II)$_2$, CH_3O^-, and **4**)[33] into a ternary complex that is stabilized by −13 to −15.5 kcal/mol relative to the free energies of the noncomplexed partners. Placing the ternary complex (or its kinetic equivalent, for example **1**-Zn(II)$_2$:**4**$^-$) into a deep thermodynamic well does little for promoting the cyclization of **4** unless the transition state for the catalyzed reaction is stabilized to a greater extent. As shown in column 5 of the Table, the $\Delta G^{\ddagger}_{cat}$ values for the cylcization of the bound substrates are endothermic by ∼13−17 kcal/mol such that the transition-state energy for the catalyzed reaction is 21−23 kcal/mol lower than the transition-state energy for the methoxide-catalyzed cyclization. Put another way, the stabilization energy associated with the binding of **1**:Zn(II)$_2$ to the [CH_3O^-:**4**]‡ transition state is −21 to −23 kcal/mol. This brings the free energy of the transition state for the catalyzed reactions for all the substrates to within 0 to 1.4 kcal/mol of the free energy of the ground-state components.

5. Conclusions

The remarkable catalysis of the cleavage of the RNA models **4**a−g that is exhibited by a simple system comprising **1**:Zn(II)$_2$:($^-$OCH$_3$) and a medium effect imbued by the methanol solvent stands out among all known catalytic systems for the cleavage of 2-hydroxypropyl aryl phosphates. The available data permit a detailed analysis of the change in mechanism from substrate binding to chemical cleavage of the catalyst-bound substrate as the $^{S}_{sp}pK_a$ values of the substrates' leaving groups increase. It has been pointed out[35] that enzyme active sites comprise a domain of effectively reduced dielectric constants, but at the same time are decorated with specifically oriented functional groups to create a specific medium tailored for a given reaction. Since **1**-Zn(II)$_2$ is a poor catalyst for the cleavage of phosphate diesters in water[36] but is an exceptional one in methanol, we view the net positively charged catalyst as one important component that further requires an intimately associated low dielectric constant/polarity environment in order to exert its maximum catalytic efficiency. The dinuclear complex **1**:Zn(II)$_2$ concentrates considerable positive net charge for binding, orienting, and promoting the cleavage of anionic

(33) There is a kinetic ambiguity as to whether the active form of the catalyst is **1**-Zn(II)$_2$ which binds substrate that subsequently undergoes deprotonation by external methoxide, or whether the active form is **1**-Zn(II):($^-$OCH$_3$) which binds substrate that undergoes a spontaneous decomposition to cyclized product mediated by the "internal" methoxide. Although these routes are kinetically equivalent and thus thermodynamically equivalent, we prefer the **1**-Zn(II)$_2$:($^-$OCH$_3$) formulation due to its simplicity in recruiting the required catalytic components into one entity and the fact that the reaction conditions where there is optimal reactivity require a **1**:Zn^{2+}:$^-$OCH$_3$ ratio of 1:2:1.

(34) Energies of activation calculated from the Eyring equation as $\Delta G^{\ddagger} = -RT \ln(k_{cat}/(kT/h))$.

(35) Richard, J. P.; Ames, T. L. *Bioorg. Chem.* **2004**, *32*, 354.

(36) Kim and Lim (ref 12) have reported that the cleavage of bis-(2,4-dinitrophenyl)phosphate promoted by **1**:Zn(II)$_2$ in water as a function of pH is not markedly different from the catalysis afforded by the mono-Zn(II) complex of 1,5,9-triazacyclododecane, the rate constant for the former being $7 \times 10^{-3}\ M^{-1}\ s^{-1}$ at pH 7. In contrast, we have found that the second-order rate constant for methanolysis of the far less reactive substrate bis-(*p*-nitrophenyl)phosphate promoted by **1**:Zn(II)$_2$:($^-$OCH$_3$) is 20 $M^{-1}\ s^{-1}$. Brown, R. S.; Lu, Z.-L. Unpublished results.

phosphate substrates. A synergistic medium effect in methanol obviously enhances the catalysis in a number of possible ways including desolvation of the ionic components, increasing the energy of interaction of the oppositely charged reaction partners, and stabilizing charged dispersed transition states relative to charge localized reactants, but more work is required to delineate these and other modes of action.

It has been pointed out[8] that enzymes that promote the cleavage of phosphodiesters[37] have k_{cat}/K_M values typically in the range of 10^6-10^7 M^{-1} s^{-1} and so provide ~20 kcal/mol of stabilization energy to the transition state of the catalyzed reaction relative to that of the background reaction. Energetics calculations of the catalysis of the cyclization of **4**a promoted by complex **5** in water originally presented by Morrow and Richard[8] indicated that the $\Delta G_{stab}^{\ddagger}$ for **5** and hydroxide-promoted cyclizations was −9.3 kcal/mol or ~50% of what could be expected of the highly evolved and efficient protein catalysts.[38] In the present case the $\Delta G_{stab}^{\ddagger}$ of −21 kcal/mol for **1**-Zn(II)$_2$:($^-$OCH$_3$)-promoted cyclization of **4**a in methanol would appear to have approached that which is maximally expected for such efficient enzymes, bearing in mind that the two catalysts operate in different media. The present model system suggests that a considerable enhancement in efficiency can be realized by a synergistic tailoring of the catalyst and medium in which the reaction occurs, and that this may be a general and exploitable phenomenon in the creation of man-made catalysts for the cleavage of phosphoesters and related materials.

(37) Raines, R. T. *Chem. Rev.* **1998**, *98*, 1045.
(38) The reader will appreciate that any catalyst offering 50% of the 20 kcal/mol of energy of stabilization of the protein system will still be 10 million times less efficient than the enzyme in terms of rate constant. See Tang, M.-Y.; Iranzo, O.; Richard, J. P.; Morrow, J. R. *J. Am. Chem. Soc.* **2005**, *127*, 1064.

Acknowledgment. We gratefully acknowledge the financial assistance of the Natural Sciences and Engineering Research Council of Canada (NSERC), The Canada Council of the Arts (CCA), and the Canada Foundation for Innovation (CFI). We are indebted to Dr. Ruiyao Wang for his expertise in solving the X-ray diffraction structure of **1**-Zn(II)$_2$:($^-$OH) and Dr. Dave Edwards for helpful discussions. In addition, S.E.B. thanks NSERC for an Undergraduate Summer Research Award, C.T.L. thanks NSERC for a PGS-2 postgraduate scholarship, and R.S.B. thanks the CCA for a Killam Research Fellowship, 2007−2009.

Supporting Information Available: Tables of pseudo-first-order rate constants for reactions of **4**b−g with **1**-Zn(II)$_2$:($^-$OCH$_3$); NMR and mass spectroscopic data for the identity of substrates **4**a−g; structural report and CIF file for **1**-Zn(II)$_2$($^-$OH)(CF$_3$SO$_3^-$)$_3$(CH$_3$OH). This material is available free of charge via the Internet at http://pubs.acs.org.

JA076847D